

LA-UR-89-1936

Los Alamos National Laboratory is operated by the University of California for the United States Department of Energy under contract W-7405-ENG-36.

TITLE: Radiographic Study for Sympathetic Detonation of 500-lb Bombs

AUTHOR(S): Dr. Roy A. Lucht, M-8

SUBMITTED TO: 1989 Flash Radiography Topical Symposium, 15-18 August 1989

8
4
4
2
0
6
3
5

By acceptance of this article, the publisher recognizes that the U.S. Government retains a nonexclusive, royalty-free license to publish or reproduce the published form of this contribution, or to allow others to do so, for U.S. Government purposes.

The Los Alamos National Laboratory requests that the publisher identify this article as work performed under the auspices of the U.S. Department of Energy.

Los Alamos Los Alamos National Laboratory
Los Alamos, New Mexico 87545

RADIOGRAPHIC STUDY FOR SYMPATHETIC DETONATION OF 500-lb BOMBS

Dr. Roy A. Lucht
Los Alamos National Laboratory
Group M-8, Explosives Applications
Mail Stop J960
Los Alamos, NM 87545
(505) 667-6617

8 4 4 2 0 6 3 6

Flash radiography techniques have determined the size and velocity vectors in the near field of fragments from tail- and side-initiated MK 82 MOD 1, general-purpose bombs. Excellent radiographs have been acquired from nine separate tests. Unlike arena tests, the radiographs were taken 75 to 125 cm from the case and show that the fragments peel off the case in long strips. A major concern in the design and execution of the experiments was the protection of the 450-kV x-ray heads and the film cassettes from fragments and blast produced by the 500-lb bombs. The velocity and size data, along with optical and electronic pin data, were used to characterize the fragments of the donor bomb in a donor-acceptor sympathetic detonation system study. The bombs were found to contain large shrink voids, randomly located from bomb to bomb, in the explosive Tritonal fill. Characteristics of the fragments from the void side of the bomb were found to be as much as 10% different from the nonvoid side and were much less reproducible than the fragments characteristic of the nonvoid side. The data collected will be useful in evaluating sympathetic detonation mitigation systems designed for use with the bombs. Such mitigation systems may be required for mass storage methods to meet the evolving insensitive munition requirements.

INTRODUCTION

The U.S. Air Force is involved in a large study of insensitive munitions, part of which includes the prevention of mass detonation of conventional munitions in storage by means of mechanical suppressants. Los Alamos has been participating in this effort since FY1986 with funds provided by AD/XR-3, Eglin Air Force Base, Florida.

BACKGROUND AND APPROACH

The MK 82 MOD 1, 500-lb bomb, a widely used general-purpose munition, contains about 87 kg of Tritonal explosive (80/20 wt%, TNT/Al) and has a variable-thickness steel case. It is not an ideal system to characterize, from an explosives viewpoint, because the Tritonal fill is not homogeneous. Large voids, produced when the Tritonal cools and solidifies, and variable explosive composition, caused by the aluminum powder settling during solidification, are typical of all the bombs we have

8 4 4 2 0 6 3 7

examined. Voids are not uniform in size or position from bomb to bomb, and the explosive composition in each bomb ranges from 70/30 wt% TNT/Al to Tritonal to pure TNT crystals. We concentrated our experimental effort on defining the effect that the presence of this void, the lack of uniform explosive composition, and the initiation point have on fragment velocity and size.

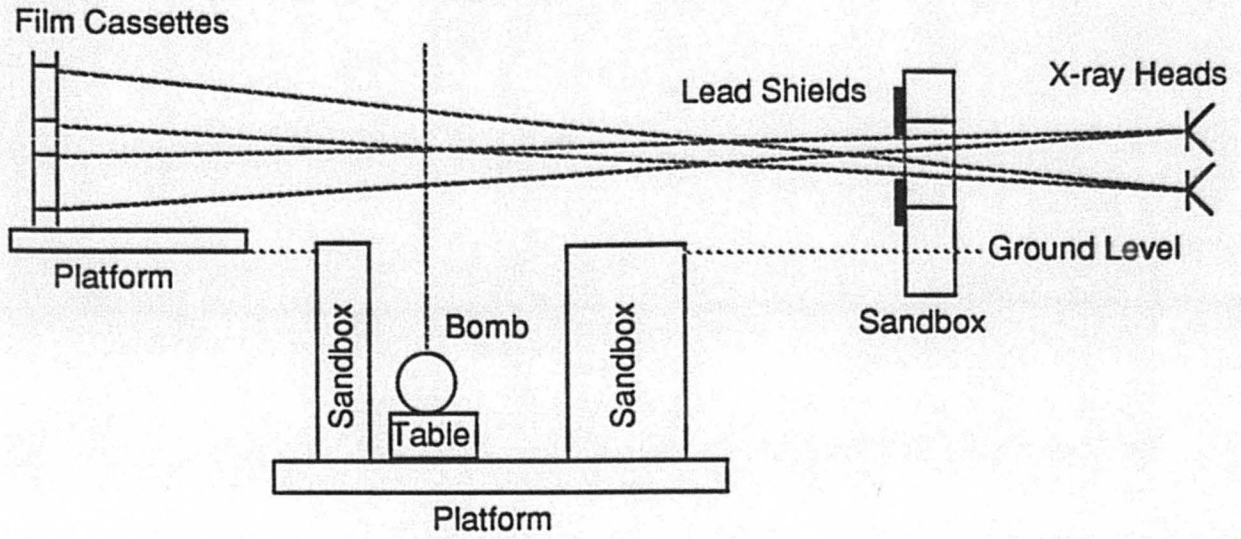
Our overall approach to the MK 82 bomb mass detonation problem is to establish the reaction thresholds of the bomb to shock, fragment attack, and mechanical damage. We can then evaluate candidate suppressant systems as to their ability to reduce the donor bomb threat levels to values well below the established thresholds. Although many shots have been fired with MK 82 bombs over the years, there appears not to have been a systematic evaluation of the fragments produced and their velocities, other than of the terminal observations provided by arena tests. Our approach is to characterize the MK 82 fragment pattern and velocity from the void and nonvoid sides, when the bomb is tail initiated. Also, in an accident situation or as a result of sabotage, there is no assurance that the donor will be tail initiated. Thus we must define the worst-case initiation point for donor fragment and shock production. We performed several two-dimensional hydrodynamic calculations, which showed that initiation of the bomb perpendicular to its axis on the outside surface should produce the most lethal shock and fragments. Thus our characterization effort included side-initiated MK 82 bombs.

EXPERIMENTAL TECHNIQUE

Three main classes of diagnostics were used: x radiography, timing pins, and fast optical photography. Radiography was the main diagnostic, and protecting the x-ray heads and film cassettes was the main challenge. Figure 1 shows a schematic of the setup as well as a photograph taken just before a radiographic shot. At the far right, behind the sandbags, are the 450-kV Hewlett-Packard x-ray heads that operate remotely from the Marx banks (beyond the picture). The sandbox to the right center protects the x-ray heads and holds the lead shades separating the two beams. In the center of Fig. 1 is the bomb, held on a wooden table well below ground level, surrounded by sandboxes to protect equipment from fragments. At the far left are the x-ray film cassettes. Each cassette frame was constructed using 100-mm steel channel. Inner dimensions were 310 mm by 740 mm. A 12.7-mm-thick aluminum sheet was used for the cassette face, and 12.7-mm-thick steel sheet with welded-angle stiffening ribs was used for the back. The 305-mm by 710-mm film pack was compressed in the center of the 100-mm-thick cassette using several layers of low-density foam. Each film pack typically consisted of a 1.6-mm-thick aluminum sheet, a QIII fluorescent screen, a sheet of NDT 57 film, QIII screen, opaque paper, QIII screen, NDT 57 film, TI 3 screen and 1.6-mm-thick aluminum. Film pack edges were double-taped with black masking tape. Occasionally, XAR film was used, although all film/screen combinations used provided excellent exposure and resolution. A sheet of Plexiglas is placed at a 45° angle to the cassettes to deflect the blast wave. The sandbags behind the cassettes slow the cassettes after they are launched by the bomb blast. Although the cassettes flew 30 to 150 m, they were not damaged and no film was lost during the 12 radiographic tests. The bombs were tail initiated by Composition C that was packed 6 in. deep in the fuze well; side initiated with a 2-in.-diam by 2-in.-long piece of PBX 9501,* or side initiated with a TOW II shaped

* PBX 9501: HMX/Estane/BDNPA-F: 95%/2.5%/2.5% by weight

MK 82 Bomb Shot Design



MK 82 Bomb Shot Setup



Figure 1. MK 82 bomb shot design schematic and photograph of a preshot setup.

8 4 4 2 0 6 3 8

charge. Two dynamic radiographs were taken of most shots about 100 μ s apart. The times were chosen so that the radiographs were taken after the bomb case was completely fragmented and the maximum fragment velocity was attained. The two radiographs allowed us to record the bomb fragments at two distinct times and displacements, from which the fragment velocity and direction could be determined. Static radiographs with fiducials and careful setup measurements were made before each shot so that the fragment displacements could be accurately determined.

To orient the bombs appropriately for each test, voids were located before the dynamic events using radiographs taken with a 25-MV betatron. Orthogonal views were taken of every bomb, and an example is shown in Fig. 2. The void/low-density area seen in this bomb is typical of all those examined. However, the void location and specific shape of the void are different for each bomb. Several radiographs must be taken to cover the entire bomb, so Fig. 2 is a composite of five individual radiographs plus the center orthogonal view.

The second kind of diagnostic equipment used was timing pins. Two types were used. First, we were interested in detecting initial motion of the bomb case to verify that the bomb being tested detonated high order and to see if the initial motion was different on the void and nonvoid sides. Thus most of our tests included linear electronic pin arrays that allowed us to record a phase velocity down the bomb axis. These pins were located on the outside surface of the bomb case at known distances from the tail, and they shorted (producing a timing signal) when the shock wave first

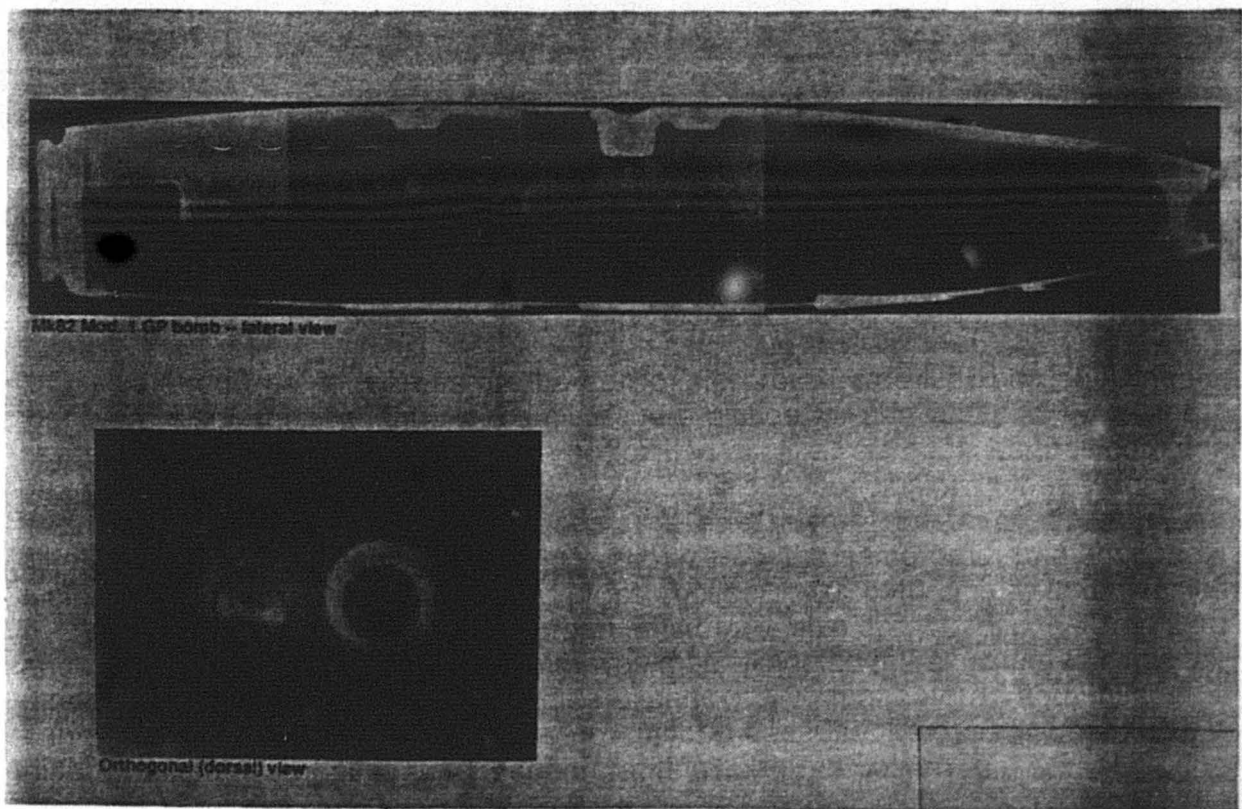


Figure 2. Static radiograph of MK 82 bomb showing void as the dark region in the lower half of the bomb.

8 4 4 2 0 6 4 0

moved the case. Secondly, we used hexagonal arrays of electrical capped pins on two shots to record the first few centimeters of bomb case expansion. Each pin was at a known distance from the initial bomb surface so that a distance-time profile could be plotted from the pin closure times. Three arrays were used on each shot to sample case motion over both the void and nonvoid sides.

Finally, two types of visible light photography were used for the third diagnostic. Four shots were fired using a smear camera and an image intensifier camera (I²C) array to optically evaluate case motion on the void and nonvoid sides of the same bomb. The shots were back-lighted so that the shadow of the expanding case followed by the expanding gas cloud was imaged on film. The smear camera provided time/distance expansion profiles, whereas the I²C array provided 30-ns snapshots at intervals during the expansion. The smear camera experiments were essentially equivalent to a standard copper cylinder test used to evaluate explosive energy, but with a full-up bomb instead.

RESULTS

Examples of dynamic radiographs from one tail- and one side-initiated shot are shown in Figs. 3 and 4, respectively. Tables I and II are fragment velocity data taken from the radiographs shown in Figs. 3 and 4. Five good radiographic experiments were completed for tail-initiated shots, four for side-initiated shots with PBX 9501, and one for side-initiated shots with a TOW II shaped-charge warhead. Several comments can be made about the radiographic data. Because the fragments are from an expanding cylinder, only the leading fragments radiographed can be assumed to have a low- or zero- "Z"-velocity component. In this Cartesian coordinate system, the "X" and "Y" components define a vertical plane through the bomb axis, where "X" is parallel to the bomb axis, "Y" is vertical, and "Z" is parallel to the direction of x-ray beam propagation. Thus, for the radiograph to be useful, it is mandatory that the leading-edge fragments are identifiable in both exposures.

The data include fragment cross-sectional areas from both views (i.e., both x-ray exposures in a given experiment), velocities in the "X" and "Y" directions, total velocities, and trajectory angle. Because the fragments are irregularly shaped and tumbling, the cross-sectional areas can be considerably different at the two times viewed in the experiment. Many of the fragments are at least 10 cm long. The area values indicate the visible range of sizes. No obvious large difference is seen between the observed fragments from the void and nonvoid sides or from the tail- and side-initiated bombs.

However, the analyses included some very small, fast fragments and some well below the leading edge, where they may have significant "Z"- component velocities that cannot be resolved. It is more reasonable, when we compare void- and nonvoid-side performances, to consider only fragments representing large leading-edge fragment motion. Because they are large, these fragments best represent the bomb case motion and have the most consistent velocities. Thus we performed another analysis in which the large leading-edge fragments were chosen without regard to fragment velocities and the results were averaged. This is shown in Table III.

8 4 4 2 0 6 4 1

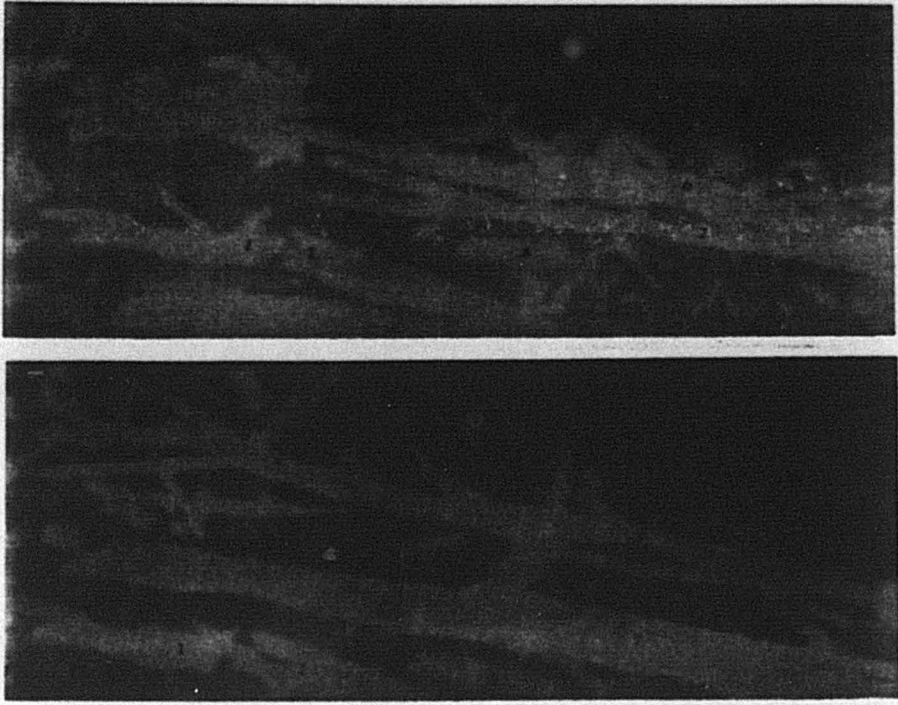


Figure 3. Dynamic radiographs of tail-initiated MK 82 bomb fragments from the nonvoid side. Radiographs are separated by 96 μ s.

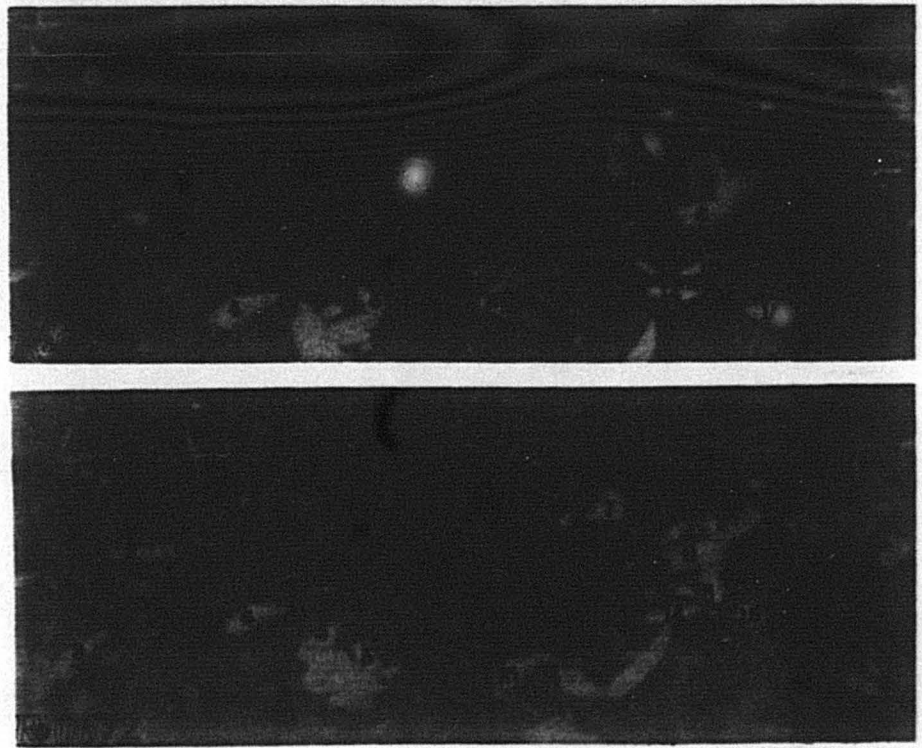


Figure 4. Dynamic radiographs of side-initiated MK 82 bomb fragments from the void side. Radiographs are separated by 80 μ s.

8 4 4 2 0 6 4 2

TABLE I
FRAGMENT AREAS, VELOCITIES, AND ANGLES
FOR A TAIL-INITIATED SHOT

Fragment Number	Film I Area (cm ²)	Film II Area (cm ²)	V(x) (mm/μs)	V(y) (mm/μs)	V (mm/μs)	∅ (°)
1	21.50	21.68	0.25	2.09	2.11	6.80
2	9.19	7.86	0.06	2.17	2.17	1.67
3	5.27	3.35 ^a	0.24	1.96	1.97	6.96
4	3.36	2.70	0.29	1.71	1.73	9.55
5	3.20	5.51	0.38	1.85	1.88	10.96
6	6.44 ^b	4.42 ^b	0.26	1.82	1.84	7.98
7	6.46 ^b	6.72 ^b	0.50	1.97	2.04	14.18
8	12.56 ^a	13.72	0.22	2.21	2.22	5.64
9	0.71	0.89	0.37	2.05	2.09	10.08
10	3.22	5.20	0.24	1.85	1.86	7.33
11	2.23	3.43	0.14	1.84	1.85	4.34

^a Off edge of film.

^b Long-fragment, arbitrary cutoff point.

$$V(av) = 1.98 \pm 0.156 \text{ mm}/\mu\text{s}$$

$$\emptyset(av) = 7.77 \pm 3.392^\circ$$

TABLE II
FRAGMENT AREAS, VELOCITIES, AND ANGLES
FOR A SIDE-INITIATED SHOT

Fragment Number	Film I Area (cm ²)	Film II Area (cm ²)	V(x) (mm/μs)	V(y) (mm/μs)	V (mm/μs)	∅ (°)
1	1.07	0.95	-0.19	2.06	2.07	-5.36
2	2.64	2.02	-0.21	2.02	2.03	-5.93
3	2.04	1.61	-0.30	1.79	1.81	-9.50
4	2.96	3.61	-1.01	1.84	2.09	-28.69
5	1.66	1.85	-0.07	2.23	2.13	-1.79
6	7.12	7.11	0.00	2.1	2.1	0
7	2.51	3.10	-0.14	2.12	2.13	-3.83
8	0.97	1.11	0.01	2.93	2.93	0.17
9	2.38	1.29	-0.01	2.15	2.15	-0.23
10	2.50	1.54	0.06	2.19	2.19	1.51
11	1.41	1.79	-0.03	2.15	2.15	-0.67
12	5.52	5.87	-0.01	2.36	2.36	-2.21
13	1.81	1.76	-0.08	1.96	1.96	-2.26
14	1.81	1.49	-0.08	1.91	1.91	-2.26
15	1.22	1.78	0.08	1.79	1.79	2.42
16	3.80	3.64	-0.18	2.25	2.26	-4.46

$$V(av) = 2.13 \pm 0.261 \text{ mm}/\mu\text{s}$$

$$\emptyset(av) = 85.66 \pm 6.99^\circ$$

TABLE III
AVERAGE FRAGMENT VELOCITIES AND AREAS

<u>Side</u>	<u>Initiation Mode</u>	<u>Velocity (mm/μs)</u>	<u>Area (cm²)</u>	<u>No. of Fragments</u>
Void	Tail	2.215 \pm 0.005	5.37 \pm 5.48	8
Nonvoid	Tail	1.947 \pm 0.018	2.72 \pm 1.68	19
Void	Side	2.08 \pm 0.31	2.21 \pm 1.80	17
Nonvoid	Side	1.86 \pm 0.11	5.06 \pm 2.72	9

The void-side fragments essentially have velocities at least 10% larger than nonvoid-side fragments. Although this is statistically accurate, the difference is not large enough to be a major consideration when suppressant systems are being evaluated. For the tail-initiated case, this difference resulted from higher late-time pressure on the void side, compared with nonvoid side, caused by the collapse of the void and consequent collision of expansion waves. For the side-initiated case, the velocity difference is probably due to a somewhat different mechanism. For the void-up side-initiated case, the detonation comes toward the void from below and must split and pass around both sides of the void. Assuming good symmetry, the two waves trapped between the void and the case would collide above the void. This, plus the reflected shock from the collapsing void, could easily provide the higher pressure required to accelerate the void-side fragments to velocities higher than the nonvoid side.

Surprisingly, the side-initiated velocities are slightly below the tail-initiated velocities. Because the side-initiated detonation wave propagation vector is nearly orthogonal to the case, the resulting fragments might have been expected to be faster than fragments from tail-initiated bombs, where the vector is almost parallel to the surface. This appears not to be the case. Whether or not the differences are statistically significant, they are too small to affect the design of any sympathetic detonation mitigation system.

Averaged fragment areas are harder to interpret. Large leading-edge fragments that were also independently discernible were picked for analysis and averaging. Larger fragments may exist but were not picked for analysis because they could not be separated from adjacent fragments. Thus the best conclusion is that typical fragments analyzed have cross sections of at least several square centimeters, and all experiment classes show fragments with sizes of the same order of magnitude. A typically large fragment could have a cross section of 20 to 40 cm², with dimensions of 2 cm by 10 to 20 cm by 0.6 cm. Fragments of this size are found in the area after a shot. The fragment thickness of 6 mm would be expected if the 10-mm-thick case stretched plastically as the bomb radius expanded 100 mm before fragmenting. Of course, thicknesses of fragments are not uniform because the case fragments at different expansion points, and it shears at angles to the bomb radii.

The smear camera and capped-pin hexagonal array results supported the radiography results of the tail-initiated bombs. Both of these types of experiments gave position-vs-time data of the early expansion of the bomb case just after the detonation wave passed. An example of the smear camera data is given in Fig. 5.

8 4 4 2 0 6 4 3

8 4 4 2 0 6 4 4

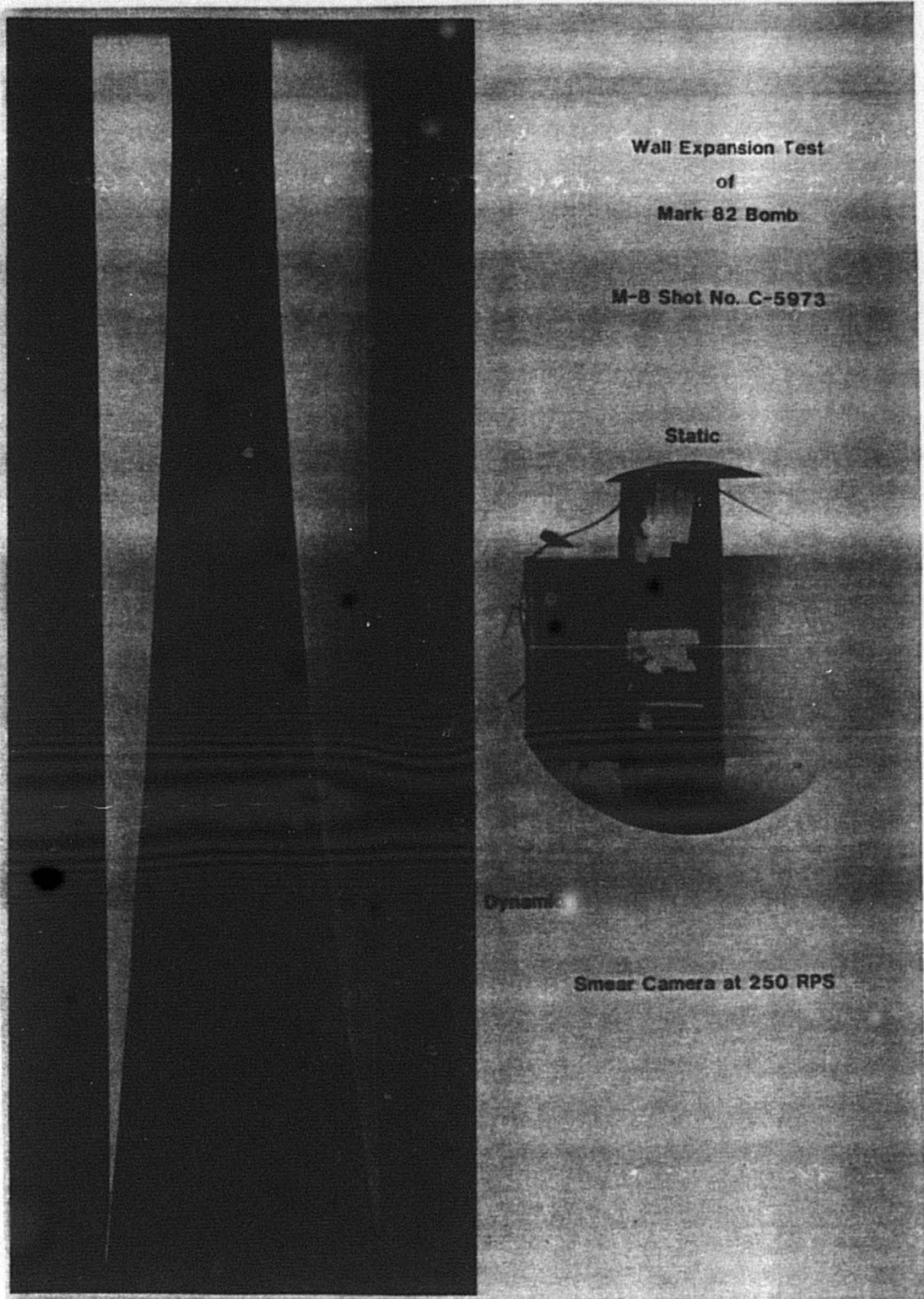


Figure 5. Smear camera record for MK 82 void and nonvoid-side case expansions. The slit is 635 mm from the bomb tail with the nonvoid side on the left and the void side on the right. The bomb was tail initiated and the tail is on top.

8 4 4 2 0 6 4 5

The static photo in Fig. 5 shows the slit positioned across the bomb diameter about halfway down the length of the bomb. A rotating mirror, in essence, sweeps the film past the slit as the bomb case expands giving the dynamic result shown in Fig. 5. The results of an analysis of a single smear camera experiment are plotted in Fig. 6, along with all hexagonal array capped-pin data and copper cylinder data from Slape et al. (ref. 1). These are scaled to the bomb geometry using the Gurney equations (ref. 2). All nonvoid-side data are consistent and all void-side smear camera data are consistent. Hexagonal pin array void-side data from one shot are consistent with all the smear camera data; however, void-side data of a second shot fall above the nonvoid-side curve of the smear camera data. Because the location and size of the void in the bomb are so nonreproducible, void-side expansion can be expected to vary greatly from bomb to bomb and from spot to spot for a given bomb.

The physical processes creating the pressure that drives the bomb case for the tail-initiated bombs can be interpreted from the smear camera data. On the nonvoid side, the detonation wave is fully supported and creates a high pressure at the steel case as it passes. This high pressure is maintained by the large bulk of explosive behind the steel case. The case is initially at rest and thus starts to move with infinite acceleration. The acceleration drops slowly but continuously as the expansion of the detonation products proceeds and the pressure correspondingly drops. On the void side, something quite different is happening. The initially high acceleration should be

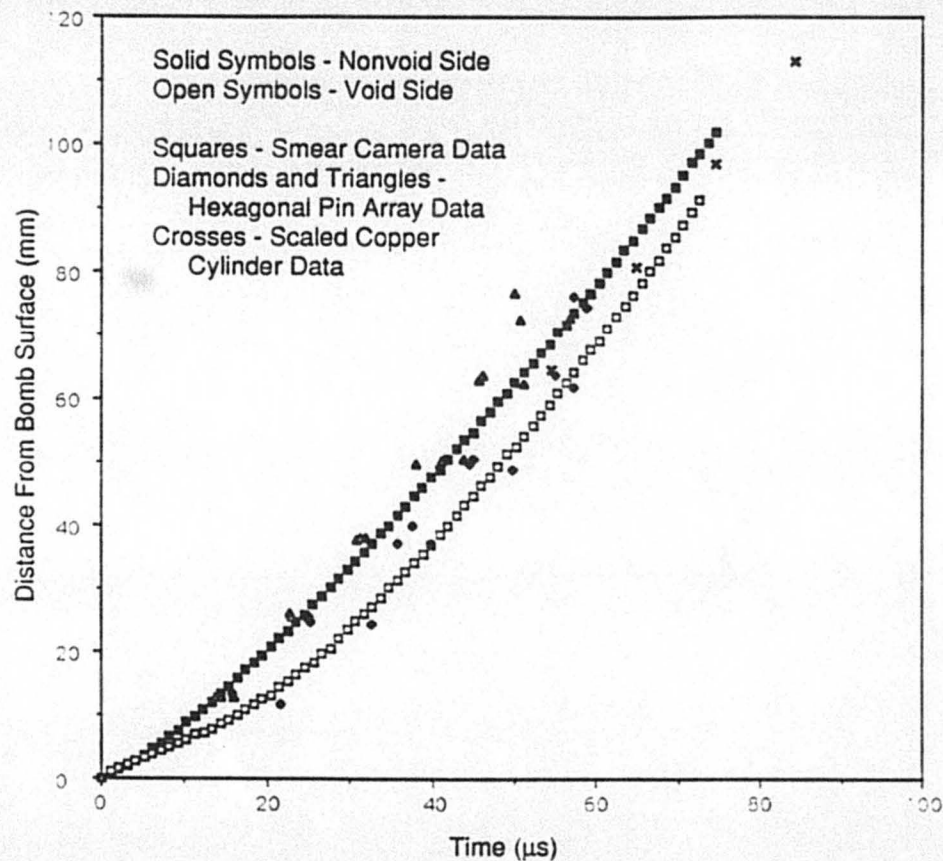


Figure 6. Smear camera, capped-pin-array, and scaled copper cylinder data.

of short duration because the gaseous detonation products can expand into the void, dropping the pressure. Case expansion then proceeds at a slower rate for a while. The products expanding into the void will collide with products from explosive from the other side of the void (the center of the bomb), causing the wave to reflect and the pressure to increase greatly. This high-pressure region then expands and catches up to the case causing significant late-time acceleration. This is precisely the behavior seen in the data (see Fig. 6). The data from all three smear camera shots show void- and nonvoid-side expansion overlapping (i.e., identical acceleration) for about the first 5 μs . Then the nonvoid-side case moves ahead of the void-side case until about 40 μs . Around 40 μs (depending on the void geometry of the given shot), the void-side case begins to accelerate faster than the nonvoid-side case and eventually passes it. Evidence for this is seen in the higher void-side fragment velocities measured from the flash radiographs. In addition, derivatives of least squares fits of the smear camera data evaluated at the time of fragmentation produce values of 2.188 and 1.823 mm/ μs for the void and nonvoid sides, respectively. Although the peak velocities determined from smear camera records agree very well, the fragment velocities from the radiographic data are slightly higher than these, which is understandable, because some positive acceleration can be expected even after the bomb case fragments. Acceleration stops or becomes negative only after the detonation products pass the fragments and produce equal pressure on all sides.

Linear pin arrays were used on almost all experiments. For the tail-initiated bombs, the linear pin data provided a distance/time plot of the detonation-driven shock wave traveling down the bomb case. Each plot was remarkably linear, and the slope, corresponding to a phase velocity, proved that the bomb detonated in high order. For the side-initiated bombs, straight-line distances were calculated through the bomb between the initiation point and pins at other points on the bomb case. The slopes from the distance-time plots of these data were direct measurements of the detonation velocity in the Tritonal-filled bomb. An example is given in Fig. 7. Data from four shots have been normalized to a common time intercept. The slope of the least squares fit is 6.534 mm/ μs , which agrees well with the published Tritonal detonation velocity (Ref. 3). of 6.475 mm/ μs .

CONCLUSIONS

The characterization of the MK 82 bomb as a tail- or side-initiated donor has been completed. The fragments radiographed from tail- and side-initiated bombs show that a worst-case fragment would be about 2 by 20 by 0.6 cm, with a velocity of 2.4 mm/ μs . The initial case motion was recorded with both electronic pins and optical devices for several tail-initiated bombs. These data show that the nonvoid side has greater acceleration from about 5 mm- to 40-mm expansion, which could result in greater pressure transmitted into close objects. The bomb radius expands about 100 mm before fragmentation. Our evaluation did not reveal any significant differences in fragment sizes or velocities caused by void location or initiation point.

ACKNOWLEDGMENTS

Many scientists and technicians contributed to this work, and the major contributors in Los Alamos Group M-8 are listed here. Richard Garcia was Firing-Site Leader for the flash radiography experiments. He was assisted by Walter Quintana

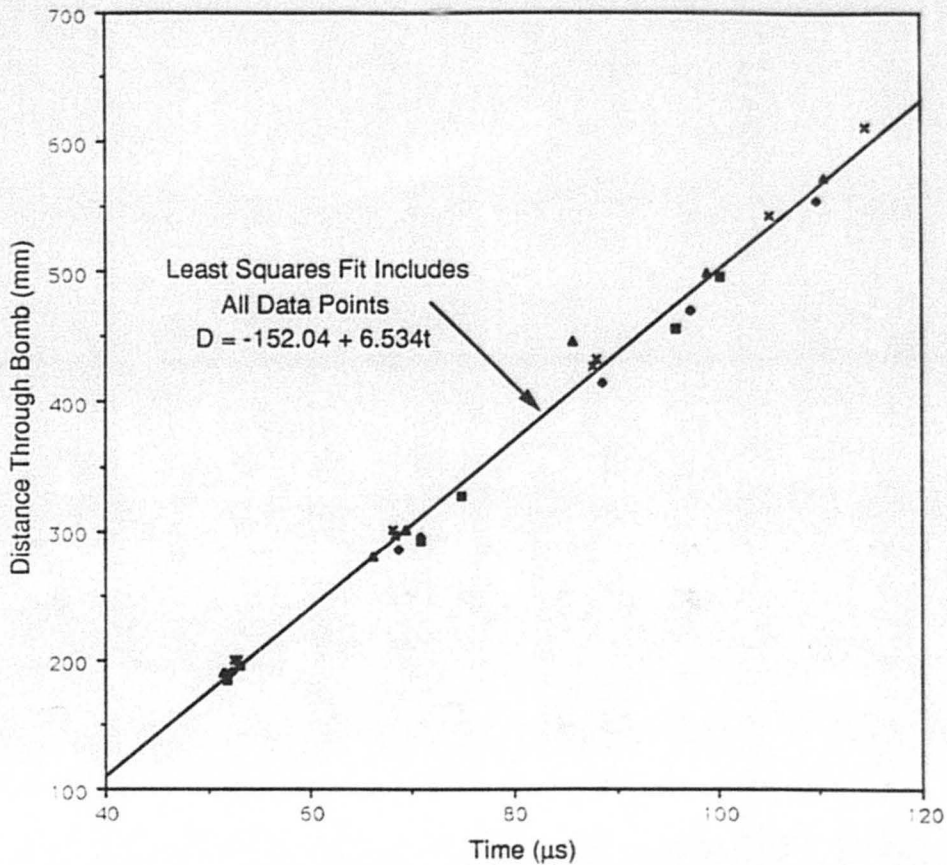


Figure 7. Nonvoid data from linear pin arrays from four experiments with time bases from individual sets adjusted to have a common time intercept.

and Max Avila. Dan Hughes was Firing-Site Leader for the smear camera experiments and was assisted by Tommy Herrera and Ken Uher. Jerry Langner analyzed the radiographs for fragment velocity and size, and Warner Miller read the smear and image-intensifier films and produced position-time data from them. William C. Davis provided the hypothesis for the difference in velocities between the void and nonvoid sides.

REFERENCES

1. R. J. Slape, J. A. Crutchner, and G. T. West, "Some Sensitivity and Performance Characteristics of the Explosives H-6 and Tritonal," AFATL-TR-74-104, Eglin Air Force Base, Florida (June 1974).
2. J. E. Kennedy, "Explosive Output for Driving Metal," **12th Annual Symposium on Behavior and Utilization of Explosives in Engineering Design**, pp. 109-124 (March 1972).
3. **Engineering Design Handbook, Explosives Series, Properties of Explosives of Military Interest** (AMCP 706-177, Headquarters, U.S. Army Materiel Command, January 1971).

Dr. Roy A. Lucht

Explosives Applications Group, M-8
Dynamic Testing Division
Los Alamos National Laboratory

Dr. Roy Lucht is the Deputy Group Leader of the Explosives Applications Group at Los Alamos National Laboratory (LANL), where he has been employed since 1975. He received a B.S. and an M.S. in Engineering Science from Florida State University in 1969, worked at NASA, Langley, until 1971 on high-powered lasers, and received a Ph.D. from Cornell University in 1975 in Applied Physics, while studying the temperature dependence of molecular energy transfer rates in chemical lasers. From 1975 through 1982, he worked at LANL on laser isotope separation of heavy metals. Since then, he has worked on explosives physics and explosive devices development, specializing in diagnostic techniques and flash x-ray use.



8 4 4 2 0 6 4 8